Supplementary Information (SI) for Journal of Materials Chemistry A.

Supplementary Information

A 7.5 V window dual-functional planar micro-device based on biopolymer ionogel electrolyte for charge storage and neuromorphic computing

Simantini Majumdar, Ann Mary Antony and Giridhar U. Kulkarni*

Chemistry and Physics of Materials Unit, Jawaharlal Nehru Centre for Advanced Scientific Research (JNCASR), Bengaluru 560064, India

***Corresponding Author.**

Email: simantini.energy@gmail.com

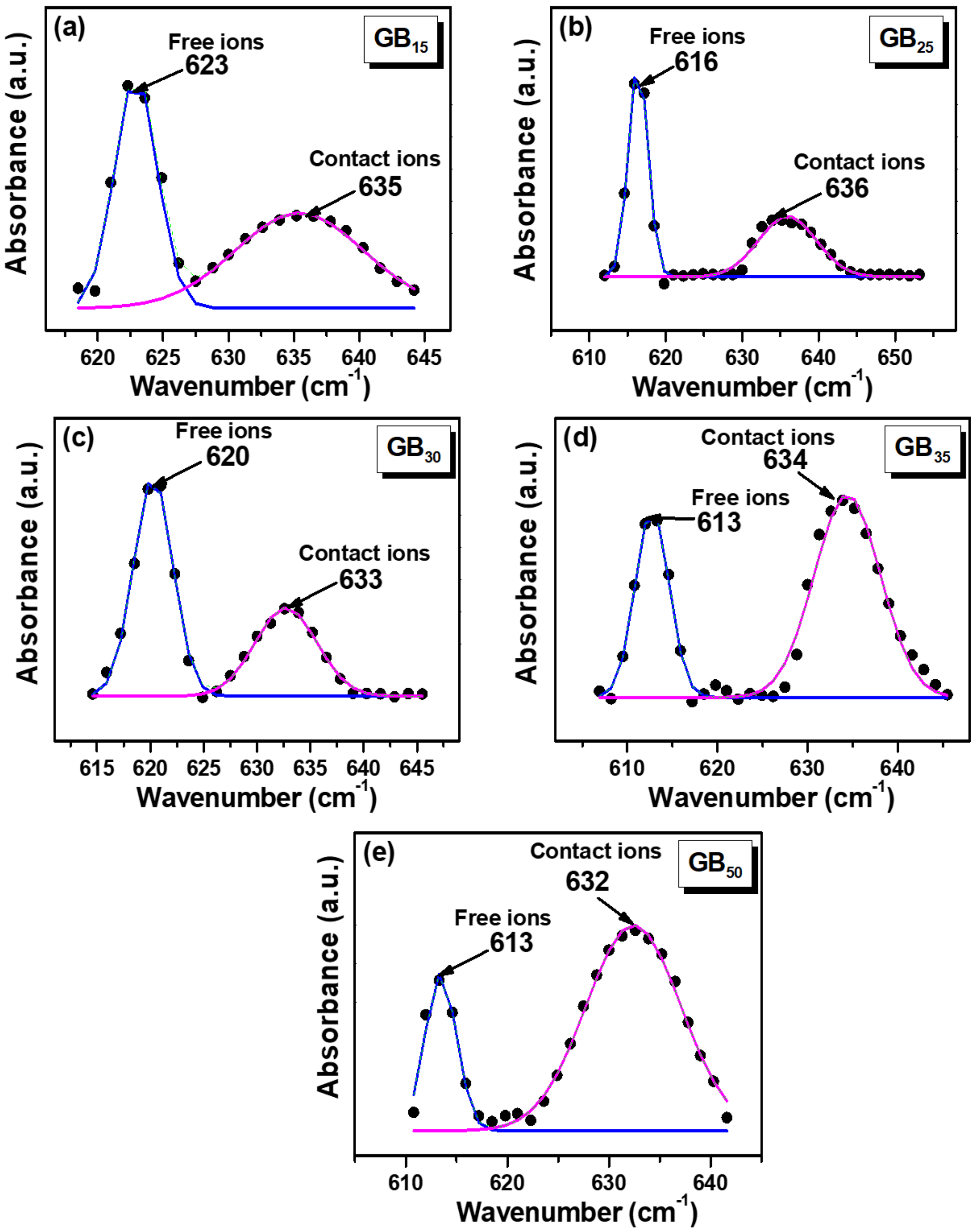

Figure S1. (a-e) FTIR absorption spectra in the region of 600 to 655 cm^{-1} for GB_x ($15 \leq x \leq 50$) blended biopolymer ionogel electrolytes with different $BMIMBF_4$ compositions. Deconvoluted FTIR absorption spectra based on Gaussian fitting function for the GB_x ionogels are represented by solid lines.

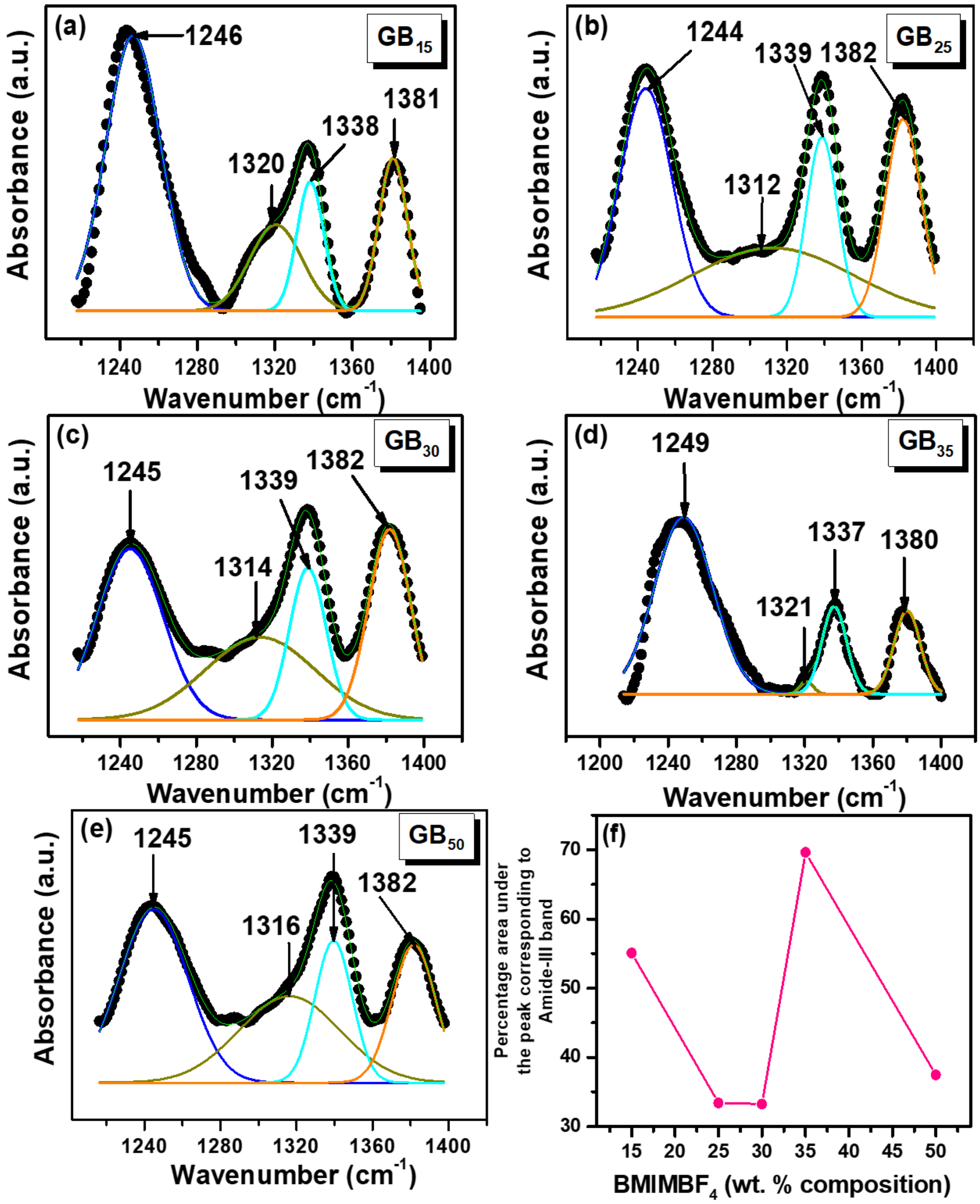

Figure S2. (a-e) FTIR absorption spectra in the region, 1200–1400 cm^{-1} for GB$_x$ ($15 \leq x \leq 50$) blended biopolymer ionogel electrolytes with different $BMIMBF_4$ compositions. Solid lines show the Gaussian fitting of the characteristic absorption peaks. (f) Percentage area under the peak corresponding to amide-III band is shown as a function of $BMIMBF_4$ doping concentrations in GB$_x$ ($15 \leq x \leq 50$) ionogels.

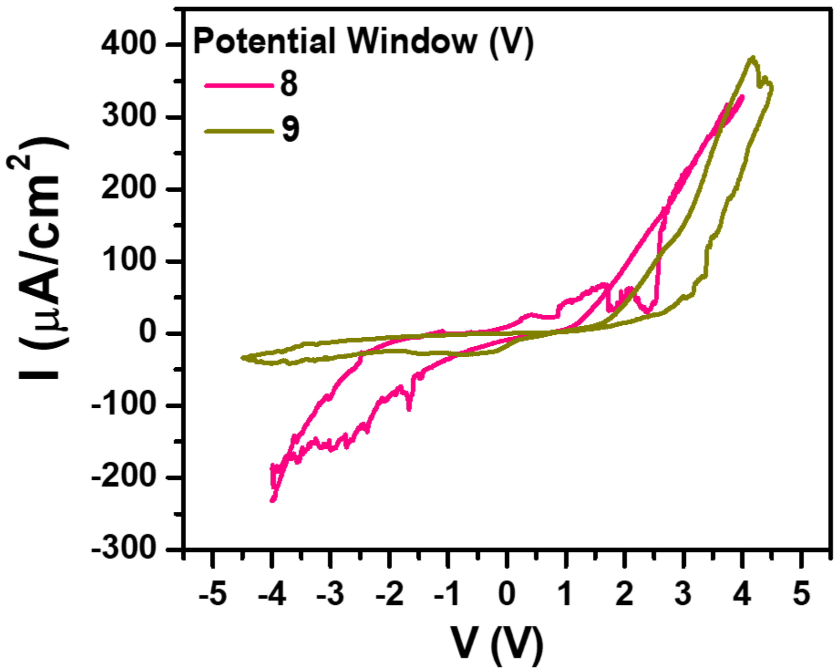

Figure S3. Cyclic voltammetry of the device measured at a scan rate of 0.1 V/s at voltage windows of 8 V and 9 V.

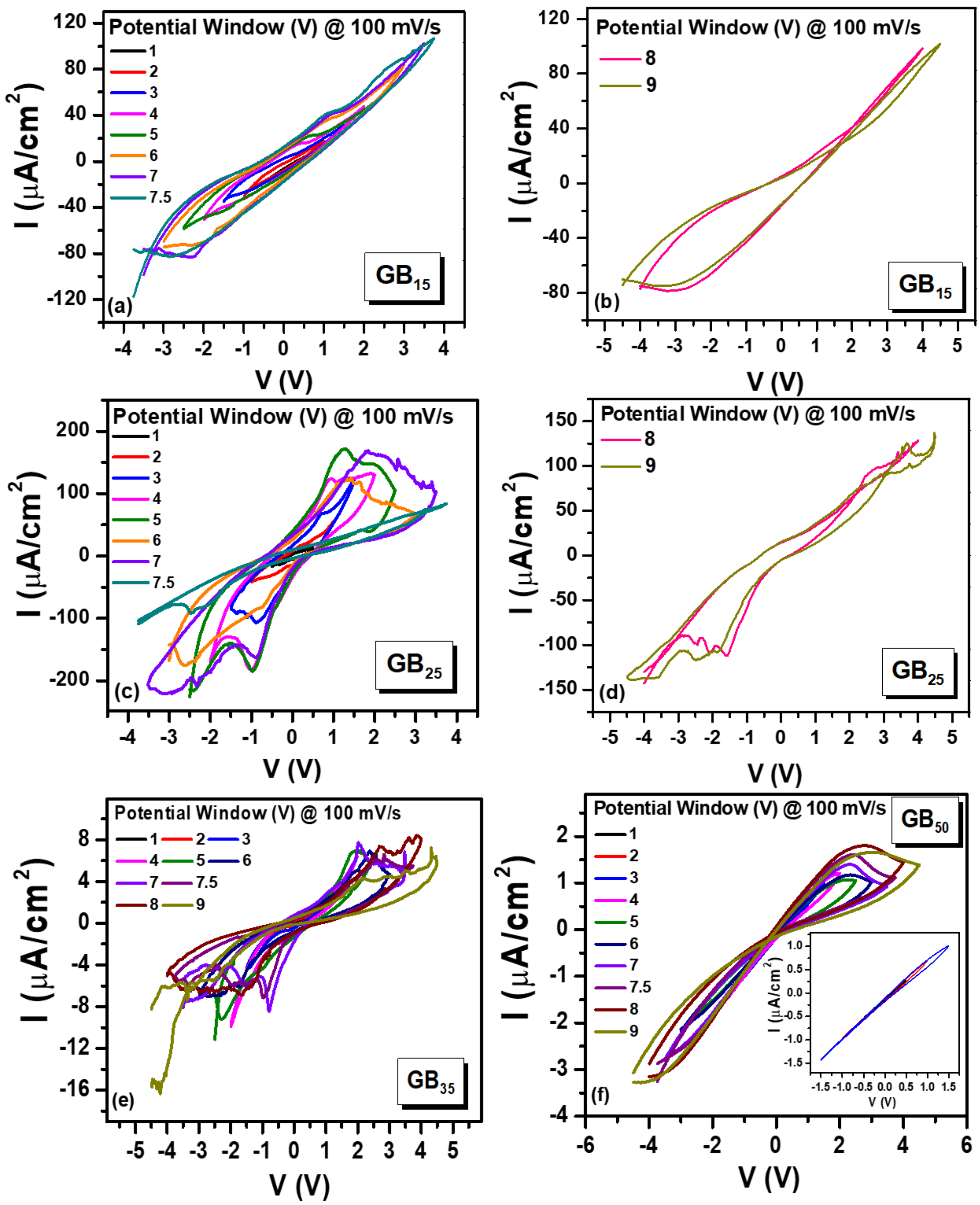

Figure S4. (a) Cyclic voltammetry of the micro-devices measured at a scan rate of 0.1 V/s at different voltage windows (1-9 V) developed with ionogels (a,b) GB_{15}, (c,d) GB_{25}, (e) GB_{35}, and (f) GB_{50}.

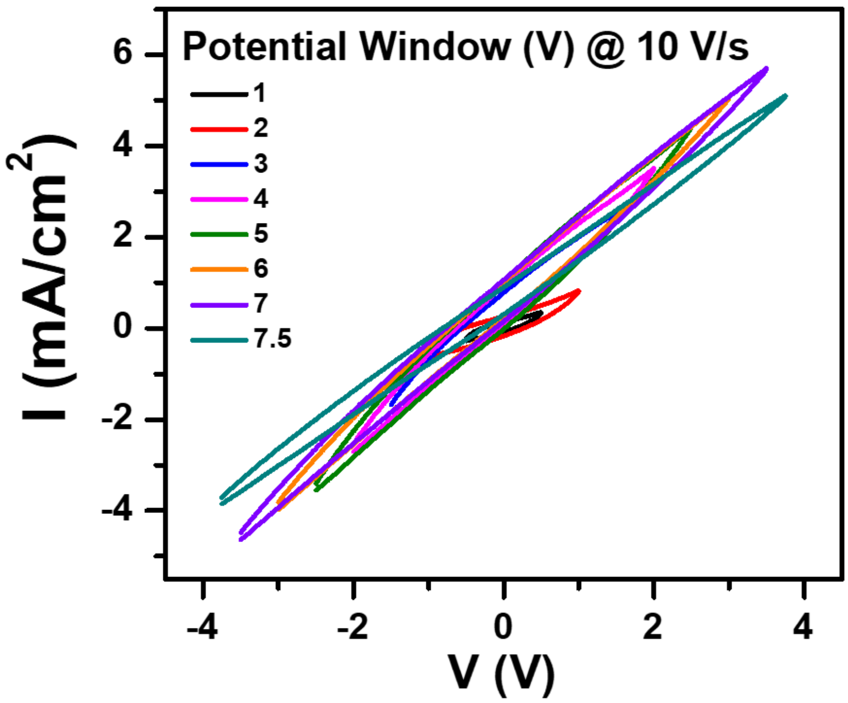

Figure S5. Cyclic voltammetry of the device measured at a scan rate of 10 V/s at different voltage windows (1-7.5 V).

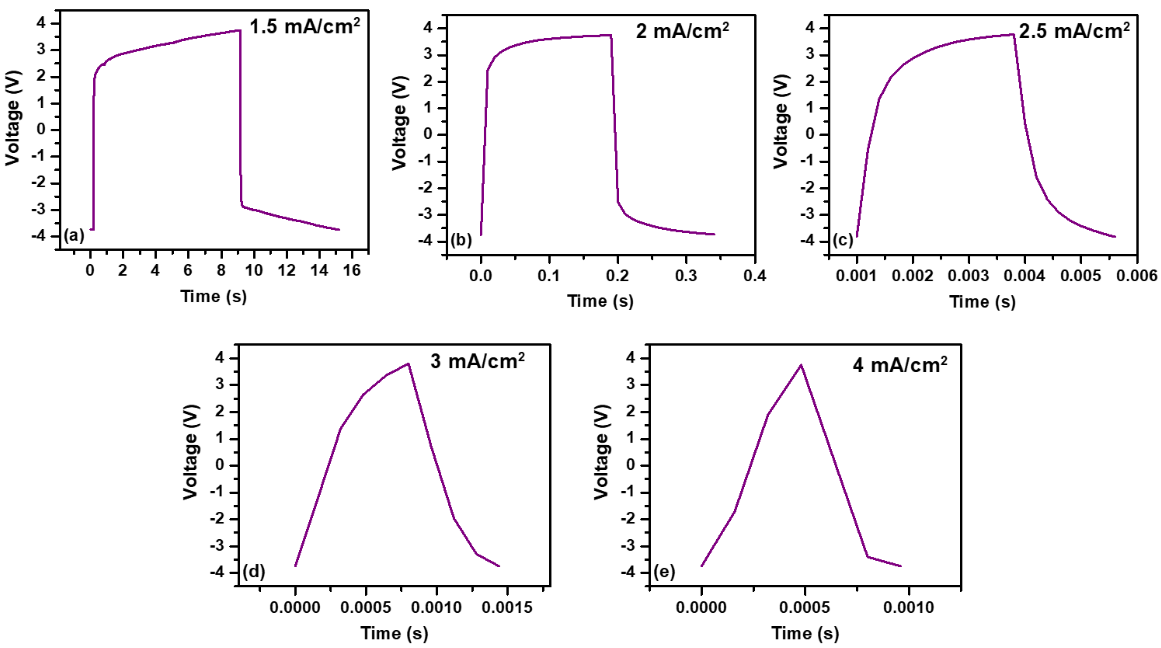

Figure S6. Galvanostatic charge-discharge for the device measured at a voltage window of 7.5 V under varying current densities, (a) 1.5, (b) 2, (c) 2.5, (d) 3, and (e) 4 mA/cm^2.

Table 1. Supercapacitive performance of CS/GL blended biopolymer ionogel electrolyte compared with other ionic liquid-based electrolyte materials.

Current Collector	Electrode Coating material	Ionic liquid-based electrolytes	ESW (V)	Capacitance	References
Aluminum foil	Polyacrylonitrile -derived porous carbon fibers (PPCF)	PVA-PAA Ionogel	2	615 mF/cm^2	[1]
Graphite paper	Activated Carbon	PAAm/ChCl/ [EMIM][TFSI]IL	2.4	43.81 F/g	[2]
Au	Vertically oriented graphene ionogel (GI)	$EMImBF_4$	4	149 µF/cm^2	[3]
Silver ink	Printed Carbon	PVA-[DPTA][BF_4]	1.2	98.8 mF/cm^2	[4]
Graphite paper	Activated Carbon	PAAM-PVA/ BMIMBr IL	1.6	284.8 mF/cm^2	[5]
Au	Activated Carbon	PIP13FSI/ PYR14FSI/ SiO_2	3	90 F/g	[6]
Aluminum foil	Carbon	AAm/ $[EMIM]^+[NO_3]^-$/ PEGDA/	2	37.35 F/g	[7]
-	3D interconnected large mesoporous carbon	PVDF-HFP /[EMI][BF_4]	4	323 F/g	[8]
None	Ionic liquid pre-intercalated MXene (PM)	$EMIMBF_4$/PVDF-HFP ionogel	3	44 mF/cm^2	[9]
Au	**None**	**CS/GL/$LiClO_4$/BMIMBF$_4$ ionogel**	**7.5**	**5.78 F/cm^2**	**Present work**

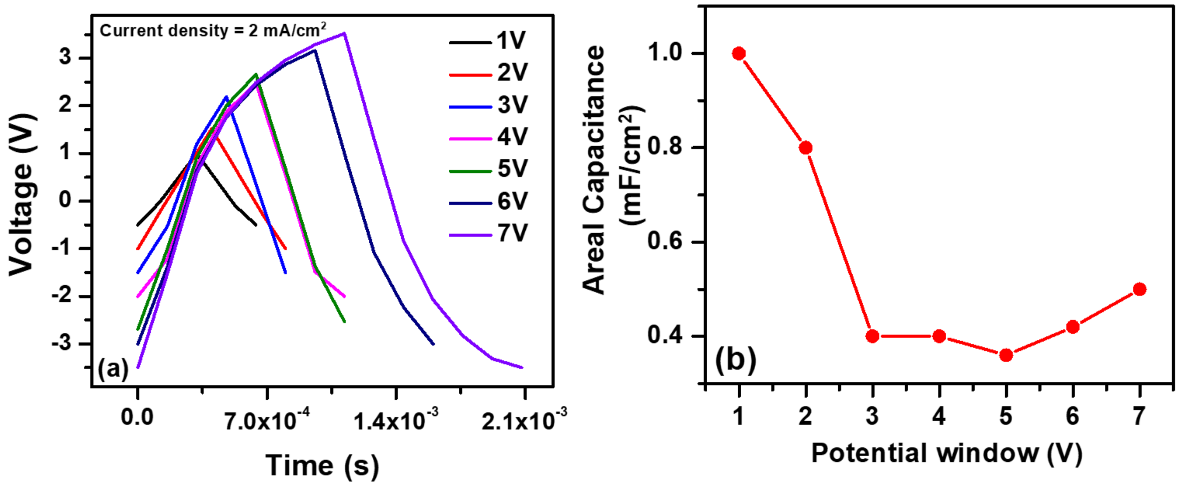

Figure S7. (a) Galvanostatic charge-discharge for the device measured at a fixed current density of 2 mA/cm^2 under varying potential windows (1-7 V), (b) Variation of areal capacitance with the potential window at a fixed current density of 2 mA/cm^2.

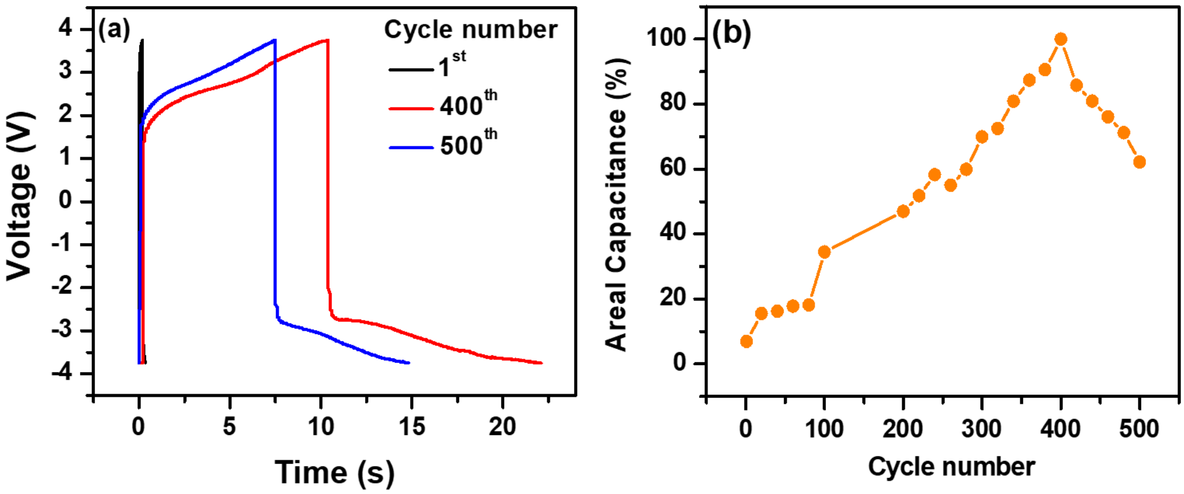

Figure S8. (a) Galvanostatic charge-discharge for the device measured at a fixed current density of 2 mA/cm^2 for 1^{st}, 400^{th} and 500^{th} cycle, (b) Cycling stability for the device over 500 cycles.

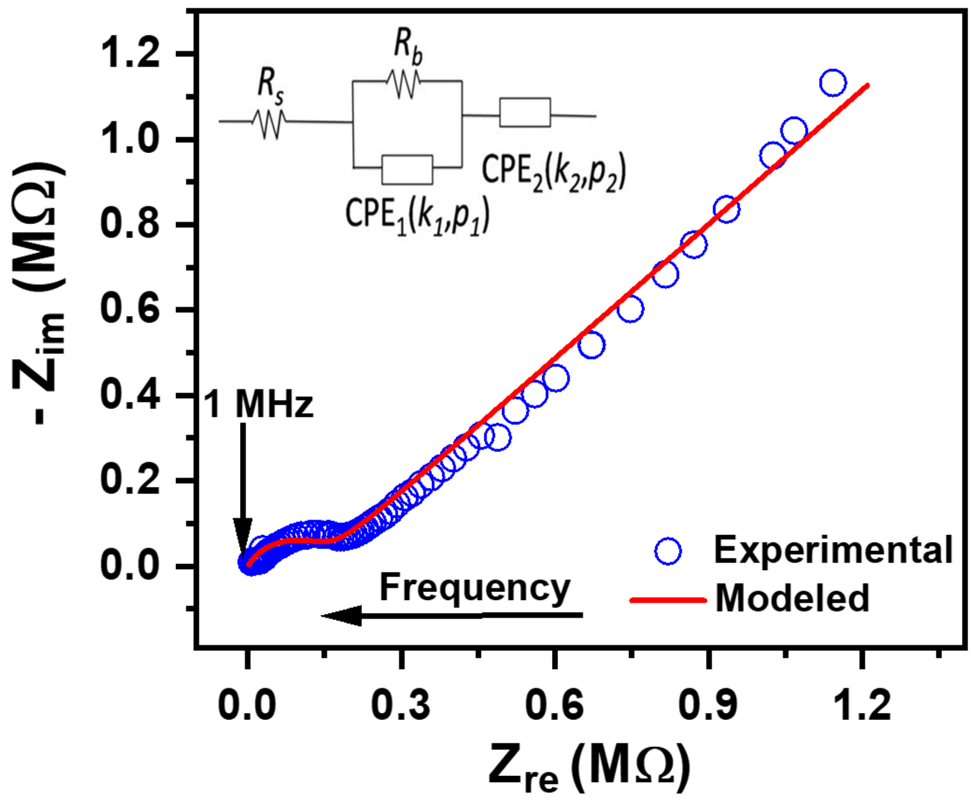

Figure S9. Nyquist plot of the device over a frequency range of 1MHz to 1 Hz, solid line represents the modelled plots based on the equivalent circuit fitting as shown in the inset.

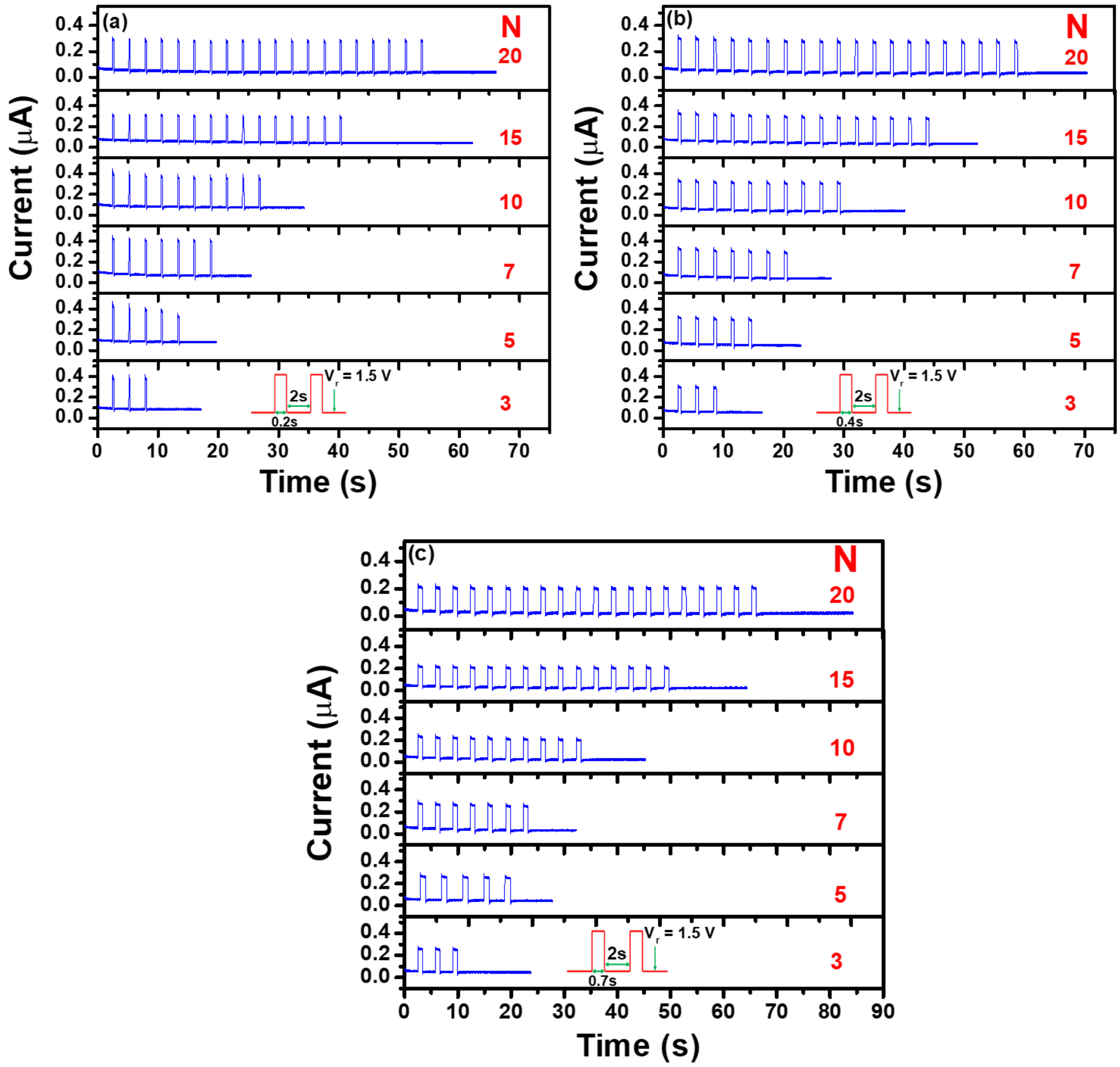

Figure S10. Synaptic behaviour emulated with pulsed voltage signals and fixed pulse interval (t_i = 2 s) with varying number of pulses (N = 3, 5, 7, 10, 15, 20) at a pulse width (t_w), (a) 0.2 s, (b) 0.4 s, and (c) 0.7 s.

References

[1] Y. Wang, Z. Wei, T. Ji, R. Bai and H. Zhu, *Small*, 2024, **20**, 2307019.

[2] G. Ma, F. Pan, X. Zhou, Z. Yong, X. Wang, C. Li, W. Bai and S. Wang, *ACS Appl. Electron. Mater.*, 2024, **6, 2**, 1434–1443.

[3] F. Chi, Y. Hu, W. He, C. Weng, H. Cheng, C. Li and L. Qu, *Small*, 2022, **18**, 2200916.

[4] A. Satheesh, S. Sushil, A. Bharathan, P. Navaneeth, P. V. Suneesh and E. Kandasamy, *Materials Letters*, 2024, **358**, 135891.

[5] Z. Yong, S. Wang, X. Wang, G. Liu, D. Liang, Y. Cui, F. Liu, D. Wang and Z. Wang, *Journal of Alloys and Compounds*, 2021, **893**, 162197.

[6] L. Negre, B. Daffos, V. Turq, P. Taberna and P. Simon, *Electrochimica Acta*, 2016, **206**, 490–495.

[7] J. Park and J-Y. Sun, *ACS Appl. Mater. Interfaces*, 2022, **14, 20**, 23375–23382.

[8] K. G. Cho, H. S. Kim, S. S. Jang, H. Kyung, M. S. Kang, K. H. Lee and W. C. Yoo, *Adv. Funct. Mater.*, 2020, **30**, 2002053.

[9] S. Zheng, C. Zhang, F. Zhou, Y. Dong, X. Shi, V. Nicolosi, Z. Wu and X. Bao, *Journal of Materials Chemistry A*, 2019, **7(16)**, 9478–9485.